

## Energy consumption in chemical-fuel driven self-assembly

Giulio Ragazzon, Leonard J. Prins\*

Department of Chemical Sciences, University of Padova, via Marzolo 1, 35131, Padova, Italy.

email: leonard.prins@unipd.it

### Abstract

Nature extensively exploits transient self-assembly structures with high energy that are able to perform work through a dissipative process. Often, self-assembly relies on the use of molecules as fuel which is consumed to drive thermodynamically unfavourable reactions away from equilibrium. Implementing this kind of non-equilibrium self-assembly processes in synthetic systems is bound to profoundly impact the fields of chemistry, materials science and synthetic biology leading towards innovative dissipative structures able to convert and store chemical energy. Yet, despite increasing efforts, the basic principles underlying chemical-fuel driven dissipative self-assembly are often overlooked, generating confusion in the meaning and definition of scientific terms which does not favor progress in the field. The scope of this Perspective is to bring closer together current experimental approaches and conceptual frameworks. From our analysis it emerges that chemical fueled dissipative processes may have played a crucial role in evolutionary processes.

Supramolecular chemistry is rapidly moving into new territory in which the composition of a dynamic system is no longer determined by the relative thermodynamic stabilities of the components, but by the capacity of the components to populate high-energy states exploiting energy-dissipating processes (Fig. 1). This capacity implies that such systems may store and transfer energy, which would bring us closer to implementing the marvelous properties of living systems in synthetic ones.<sup>1</sup> In recent years, this development has led to energy-driven molecular machines,<sup>2-7</sup> materials,<sup>8-13</sup> pattern formation,<sup>14-16</sup> and chemical reactivity,<sup>17,18</sup> which illustrate the rich possibilities offered by out-of-equilibrium chemistry. A key issue in designing out-of-equilibrium systems is the mechanism that regulates energy dissipation. Although in most cases light is used as energy source in artificial systems,<sup>19</sup> biological systems typically employ chemical energy stored in kinetically stable, high energy molecules to drive processes.<sup>20</sup> This peculiarity has sparked a strong interest in the design of chemical-fuel driven out-of-equilibrium systems, in particular related to self-assembly.<sup>11,21-36</sup> However, an examination of the reported examples shows that energy is dissipated in very different ways, but nonetheless always commonly referred to as dissipative self-assembly. This Perspective aims at providing a coherent conceptual framework to avoid confusion in terminology and be a reference point for future experimental efforts. In particular, we try to clarify the following concepts: what characterizes dissipative self-assembly and what are the design principles? How is chemical energy stored in a self-assembled system? How is dissipative self-assembly connected to dissipative adaptation?

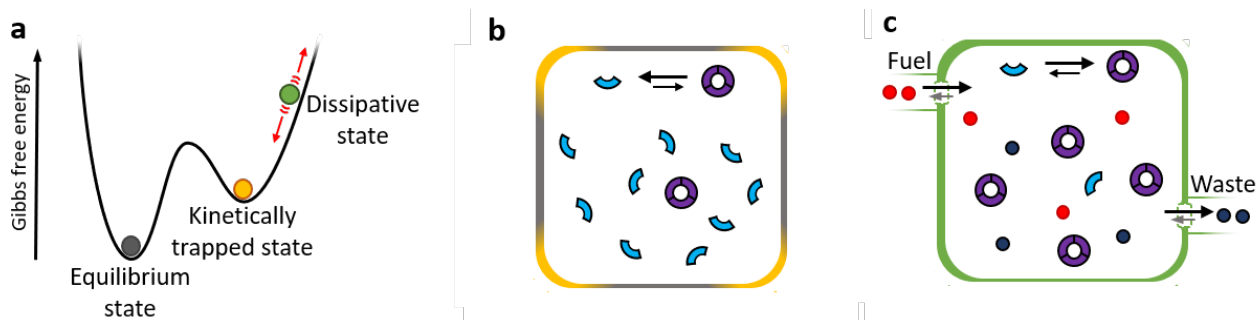


**Fig. 1 | Self-assembly at equilibrium and out-of-equilibrium.** **a**, Representation of the Gibbs free energy landscape for a generic system as a whole (*i.e.* the sum of the energy of every component), on which different situations are represented: the equilibrium state (grey circle), a kinetically trapped state (orange circle) and a dissipative state (green circle). **b**, Cartoon representation of a self-assembling system at equilibrium or in a kinetically trapped state **c**, Cartoon representation of the same system, but now in the presence of a chemical energy flux, which drives the equilibrium towards the aggregated state.

### Chemical fuel-driven self-assembly

Our considerations start with a simple self-assembly process  $nM \rightleftharpoons A_n$ , in which  $n$  monomers  $M$  may assemble to form aggregate  $A_n$ . However, this process is thermodynamically disfavored, which implies that energy is required to shift the equilibrium. Several approaches relying on the use of chemical fuels, *i.e.* thermodynamically activated molecules, have been described in the literature, differing in the way the energy stored in the fuel is transferred to the self-assembly process. We can distinguish two limiting cases.

The first case is a situation in which fuel-to-waste conversion involves neither the monomers nor the assemblies, for example when it is mediated by an external additive (*e.g.* an enzyme). Most of the reported examples that fall in this category follow the general scheme reported in Fig. 2a.<sup>21-25, 35, 36</sup> The addition of a chemical fuel ( $F$ ) to the monomer  $M$  permits the energetically downhill assembly of  $A_n^*$ . The independent conversion of fuel into waste ( $W$ ) leads to a spontaneous return of the system towards the non-assembled state in the presence of waste ( $M + W$ ). This approach is exemplified by the fuel-regulated self-assembly of vesicular nanoreactors (Fig. 2b).<sup>22</sup> In this system adenosine triphosphate (ATP) was found to template the formation of vesicles at a concentration well below the critical aggregation concentration ( $cac$ ) of the surfactant. The presence of the enzyme potato apyrase in the solution caused the gradual conversion of ATP and, consequently, a spontaneous disassembly of the vesicles occurred in time. In this case, ATP addition and enzymatic cleavage serve to regulate how much ATP is available, and the chemical equilibrium leading to assembly  $A_n^*$  adapts accordingly in a Le Chatelier-like manner. Although in these kinds of systems high energy molecules, such as ATP, are used to transiently control a self-assembly process, it is important to point out that all consumed energy (see Box 1) is just dissipated by the enzyme and never leads to population of the high-energy assembly  $A_n$ . This is a direct consequence of the fact that the assembled states ( $A_n$  or  $A_n^*$ ) never participate in fuel-to-waste conversion. As we will see next, the ability to participate in the catalytic reaction is a necessary, but not sufficient, condition to drive a self-assembly process, and maintaining it in a non-equilibrium steady state. To make the distinction with the second limiting case, we suggest reserving the term self-assembly under dissipative conditions for systems that operate according to the scheme in Fig. 2.

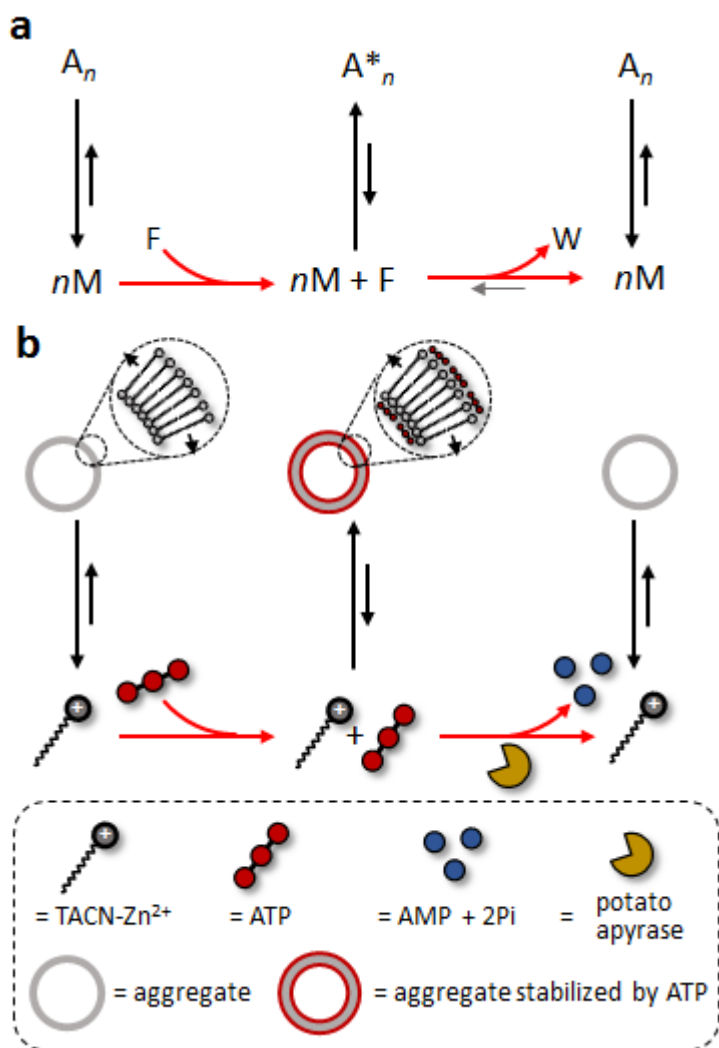


**Fig. 2 | Self-assembly under dissipative conditions.** **a**, General scheme for a self-assembling system under dissipative conditions. The association of  $n$  monomers  $M$  to give aggregate  $A_n$  is thermodynamically disfavored; in the presence of templating agent  $F$  aggregation to give  $A_n^*$  occurs in a thermodynamically favored process; upon slow depletion of  $F$ , the monomers revert to the initial situation in which  $M$  is preferentially populated. **b**, Reaction scheme for the transient assembly of vesicular nanoreactors upon adenosine triphosphate (ATP) consumption. A surfactant molecule containing  $Zn^{2+}$ -complexed 1,4,7-triazacyclononane (TACN- $Zn^{2+}$ ) as cationic head group was found to have a critical aggregation concentration ( $cac$ ) of around  $100 \mu M$ . The addition of adenosine triphosphate (ATP) resulted in the templated formation of vesicles at a concentration well below the  $cac$ . This phenomenon was attributed to the development of stabilizing electrostatic interactions between ATP and the surfactants and to preorganization of the surfactant molecules by ATP. The presence of the enzyme potato apyrase in the solution caused the gradual conversion of ATP into the waste products adenosine monophosphate and phosphate ( $AMP + 2 P_i$ ), which possess poor templating ability. Consequently, spontaneous disassembly of the vesicles occurred over time. The kinetic behavior of the system could be described with a simple model in which ATP-hydrolysis occurred only in bulk. The notation used for the components is reported in the dashed box.

### Box 1 | Terminology

The domain of non-equilibrium self-assembly brings together expertise from different areas. In some cases this has led to the attribution of different meanings to the same words. To avoid misunderstanding we define here the terminology used in this Perspective article and encourage all practitioners in the field to adopt it.

**Self-assembly under dissipative conditions:** A self-assembly process associated to chemical fuel-to-waste conversion which does not involve the building blocks.

**Dissipative self-assembly:** A self-assembly process associated to chemical fuel-to-waste conversion which is mediated by the building blocks.

**Driven self-assembly:** A dissipative self-assembly process leading to energy storage in a high-energy aggregate, as a consequence of kinetic asymmetry in energy consumption.

**Consumed energy:** the energy associated to the conversion of fuel to waste (which, at fixed [F] and [W], corresponds to an associated  $\Delta G < 0$  for the reaction). This energy is absorbed by the system and is either stored or dissipated.

**Stored energy:** the part of the consumed energy that is fruitfully exploited to shift concentrations away from their equilibrium value.

**Dissipated energy:** the part of the consumed energy that is irreversibly converted into heat and/or waste products. In line with experimental practice, the conversion into waste products is considered irreversible and in the simulations the waste is continuously removed.

The relation between the above quantities is given by the following equation:

$$\underbrace{\text{Consumed energy}}_{\text{fuel to waste conversion} \times -\Delta G} = \underbrace{\text{Stored energy}}_{\text{concentrations shift from equilibrium}} + \underbrace{\text{Dissipated energy}}_{\text{wasted energy}}$$

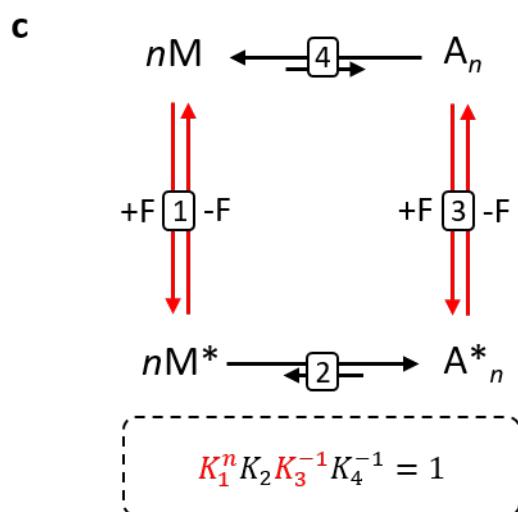
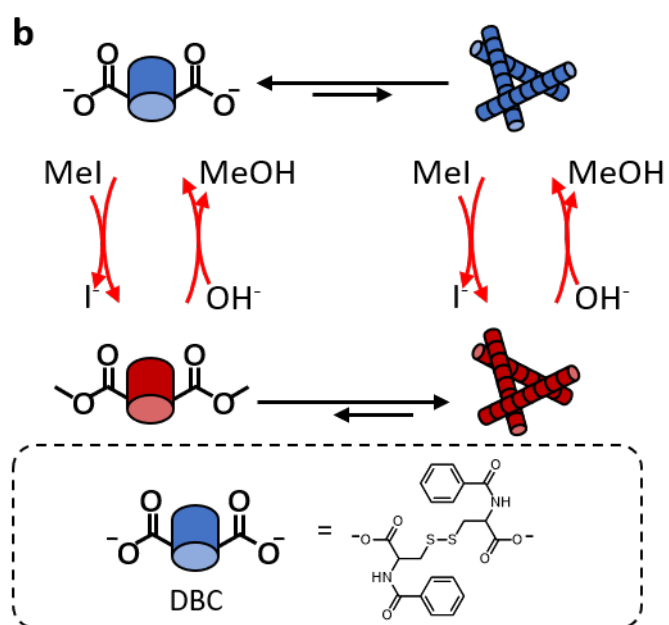
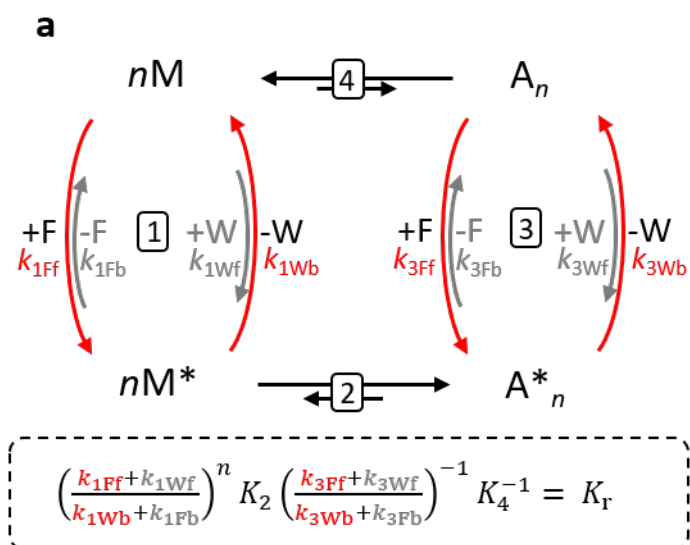


**Fig. 3 | Dissipative self-assembly a**, General scheme for a self-assembling system involved in chemical fuel consumption. The association of  $n$  monomers  $M$  to give aggregate  $A_n$  is thermodynamically disfavored; in the presence of fuel  $F$  the monomer is activated to  $M^*$  which aggregates to give  $A_n^*$  in a thermodynamically favored process. Conversion of fuel into waste  $W$  deactivates the components. The grey arrows indicate microscopic reversibility for each step. The forward constants describing fuel and waste association are pseudo-first order rate constants, because they include the fixed concentrations of  $F$  and  $W$ , as described in the SI (page 2). This observation is important, because it implies that these rate constants (and consequently  $K_r$ ) can be controlled externally by changing the fuel and waste concentrations. **b**, Reaction scheme for the transient assembly of dibenzoyl-L-cysteine (DBC) upon Mel consumption; the notation used for the components is reported in the dashed box. The arrows for the backward fuel/waste reactions are omitted for clarity reasons. **c**, General scheme for a reaction cycle analogous to that of Fig. 3a, but without fuel-to-waste conversion.  $K_1$  is defined for one monomer and, therefore, must be considered  $n$ -times in a cycle. In Figs. 3a and 3c, reaction labels are contained within boxes associated to reaction arrows, equilibrium constants are defined from top to bottom and from left to right.

A different scenario appears when energy dissipation is mediated by the self-assembling molecules (Fig. 3a).<sup>11,26-34</sup> Here, a chemical fuel (F) reacts – either covalently or noncovalently – with monomer M leading to an activated monomer M\* which has the ability to aggregate (A\*<sub>n</sub>) in a thermodynamically favored process. Contemporaneously a backward reaction takes place which converts M\* (or A\*<sub>n</sub>) back to M (or A<sub>n</sub>) accompanied by the release of waste (W). This situation is illustrated in the controlled gelation of dibenzoyl-L-cysteine (DBC) (Fig. 3b).<sup>26</sup> Above the pK<sub>a</sub> of the acidic moieties, aggregation of DBC is prevented by electrostatic repulsion. However, the addition of a methylating agent, Mel, affords the corresponding diester, which readily self-assembles into nanofibers. Under the experimental conditions, the diester is hydrolysed back to DBC causing dissociation of the aggregate. Because the hydrolysis reaction is slower than the methylation reaction, a (transient) accumulation of the diester and, consequently, of the nanofibers takes place upon the addition of fuel. In contrast with the previous scenario for self-assembly under dissipative conditions (Fig. 2), here the assembled states do play an active role in fuel-to-waste conversion. We call this situation dissipative self-assembly (Fig. 3). However, it will be shown that this condition by itself does not automatically imply that the reaction of interest is driven away from equilibrium. Indeed, it is a major objective of this Perspective to highlight that two sub-limiting cases can be identified, which differ in the way the energy is consumed by the system. In the first sub-case energy consumption occurs in a ‘symmetric’ manner as opposed to ‘asymmetric’ energy consumption in the second sub-case. It will be shown that kinetic asymmetry in the energy consumption pathways present in the system is the other necessary condition for driving self-assembly processes away from equilibrium, allowing for energy storage.

### Symmetric vs asymmetric energy consumption

To explain the difference between symmetric and asymmetric energy consumption we start with the thermodynamic equivalent of the cycle reported in Fig. 3a, in which all 4 steps are equilibrium reactions (Fig. 3c). Because of microscopic reversibility for each step, the following equation holds:

$$K_1^n \cdot K_2 \cdot K_3^{-1} \cdot K_4^{-1} = 1 \quad (1)$$

This equation implies that under stationary conditions (*i.e.* without time dependent fluctuations of any parameter of the system) a cyclic pathway 1-2-3-4 in Fig. 3c must be equally probable in the clockwise and counterclockwise direction. On the other hand, in a fuel-driven network (Fig. 3a) the activation and de-activation steps 1 and 3 occur through chemically distinct pathways, which implies that the cycle can be described by the following equation<sup>37</sup>

$$\left( \frac{k_{1Ff} + k_{1Wf}}{k_{1Fb} + k_{1Wb}} \right)^n \cdot K_2 \cdot \left( \frac{k_{3Ff} + k_{3Wf}}{k_{3Fb} + k_{3Wb}} \right)^{-1} \cdot K_4^{-1} = K_r \quad (2)$$

which differs from equation (1) in the sense that the binding constants for steps 1 and 3 have been replaced with the rate constants  $k$  for the forward (f) – and backward (b) conversion through both the fuel (F) and waste (W) pathways. Moreover, the fuel-driven cycle is connected to an exergonic reaction (F→W) which delivers energy to the system. These conditions have an important consequence, because it implies that the product of the terms in the right-hand-side of equation 2 does not have to be equal to 1. Indeed, this product can be defined as the ratcheting constant,  $K_r$ , which can be interpreted as a directionality parameter that identifies whether the systems in Fig. 3a prefers to cycle in the clockwise or counterclockwise direction. As shown in the SI (page 3), equation 2 can be further elaborated to give<sup>38</sup>

$$\left[ \frac{\left(1 + \frac{k_{1Wf}}{k_{1Ff}}\right)}{\left(1 + \frac{k_{1Wb}}{k_{1Fb}}\right)} \right]^n \left[ \frac{\left(1 + \frac{k_{3Wf}}{k_{3Ff}}\right)}{\left(1 + \frac{k_{3Wb}}{k_{3Fb}}\right)} \right]^{-1} = K_r \quad (3)$$

which nicely illustrates that the directionality of the system has exclusively a kinetic origin. The ratcheting constant  $K_r$  depends only on the ratio of the fluxes between the forward and backward paths of steps 1 and 3 and not at all on any binding constant. The observation that ratcheting originates only from an asymmetry in the transition states (and not the ground states) implies that an information ratcheting mechanism is operative.<sup>39-41</sup>

In the situation where  $K_r$  equals 1 (Fig. 3a), there is no directional preference and this cycle can be defined as ‘symmetric’. On the other hand, when  $K_r$  is greater than 1 (Fig. 3c) the system prefers cycling in a counterclockwise direction, a situation referred to as ‘asymmetric’. In the latter case, fuel preferentially activates M (as opposed to  $A_n$ ) and deactivation (leading to waste) is kinetically favored in the assembled state  $A_n^*$  (as opposed to  $M^*$ ). This kinetic asymmetry leads to a preferred pathway for fuel-to-waste conversion given by fuel activation of M to give  $M^*$ , assembly of  $M^*$  into  $A_n^*$ , and finally waste release leading to  $A_n$ . The overall reaction associated with this path is  $nM + F \rightarrow A_n + W$ . It can be clearly seen how the energy released from the exergonic conversion of fuel to waste shifts the endergonic equilibrium in the direction of  $A_n$ .

To illustrate more clearly the difference between symmetric and asymmetric dissipative cycles we have performed kinetic simulations of a simple self-assembly process (with  $n = 2$ , a detailed description is provided in the SI (page 5)). For the symmetric cycle, rate constants for the activation and deactivation pathways 1 and 3 were chosen such as to satisfy equation 2 (and 3) with  $K_r$  equal to 1. For the asymmetric cycle, we have introduced preferential monomer activation ( $M \rightarrow M^*$ ) and aggregate deactivation ( $A_2^* \rightarrow A_2$ ) by altering the involved rate constants to give a  $K_r$  value of  $1.6 \times 10^{10}$  (see below for the significance of this value). To underline the fact that driven self-assembly has a kinetic origin, we have installed preferential pathways by changing *both* the forward- and backward rates of the involved reactions to the same extent (*i.e.* without affecting the associated equilibrium constant).

Starting from an initial monomer concentration, we have followed the evolution of each system until a stationary state was reached under continuous fuel-to-waste conversion (*i.e.* at constant  $[F] = [W]$ , a condition referred to as chemostatting<sup>42</sup>). We have reported the distribution of monomer among the four states in Fig. 4a and b (indicated by the size of the green circles) for the symmetric and asymmetric cases, respectively. For the symmetric network, nearly all monomer is present in the activated aggregated state ( $A_2^*$ ), whereas for the asymmetric network the monomer resides almost completely in the deactivated aggregated state ( $A_2$ ). For each system, we then compared these distributions to those at thermodynamic equilibrium. The comparison was achieved by using the calculated steady state concentrations of all four species under dissipative conditions as input for a next simulation in which all activation and deactivation pathways (steps 1 and 3) were turned off and the system was let to equilibrate (Fig. 4a and b, grey circles). It is important to stress that in this situation conversion between the activated ( $M^*$ ,  $A_2^*$ ) and deactivated species ( $M$ ,  $A_2$ ) can no longer take place. Importantly, for the symmetric system the concentrations of all species remain equal, whereas for the asymmetric system equilibration results in a complete shift from  $A_2$  to  $M$ . This observation leads to an important conclusion: even for dissipative self-assembly systems, the fact they consume energy is not a sufficient condition to drive them out-of-equilibrium. Kinetic asymmetry in the energy consumption pathways is required to reach stationary concentrations which are different from those at thermodynamic equilibrium. Only in this case we can speak of a driven self-assembly process.

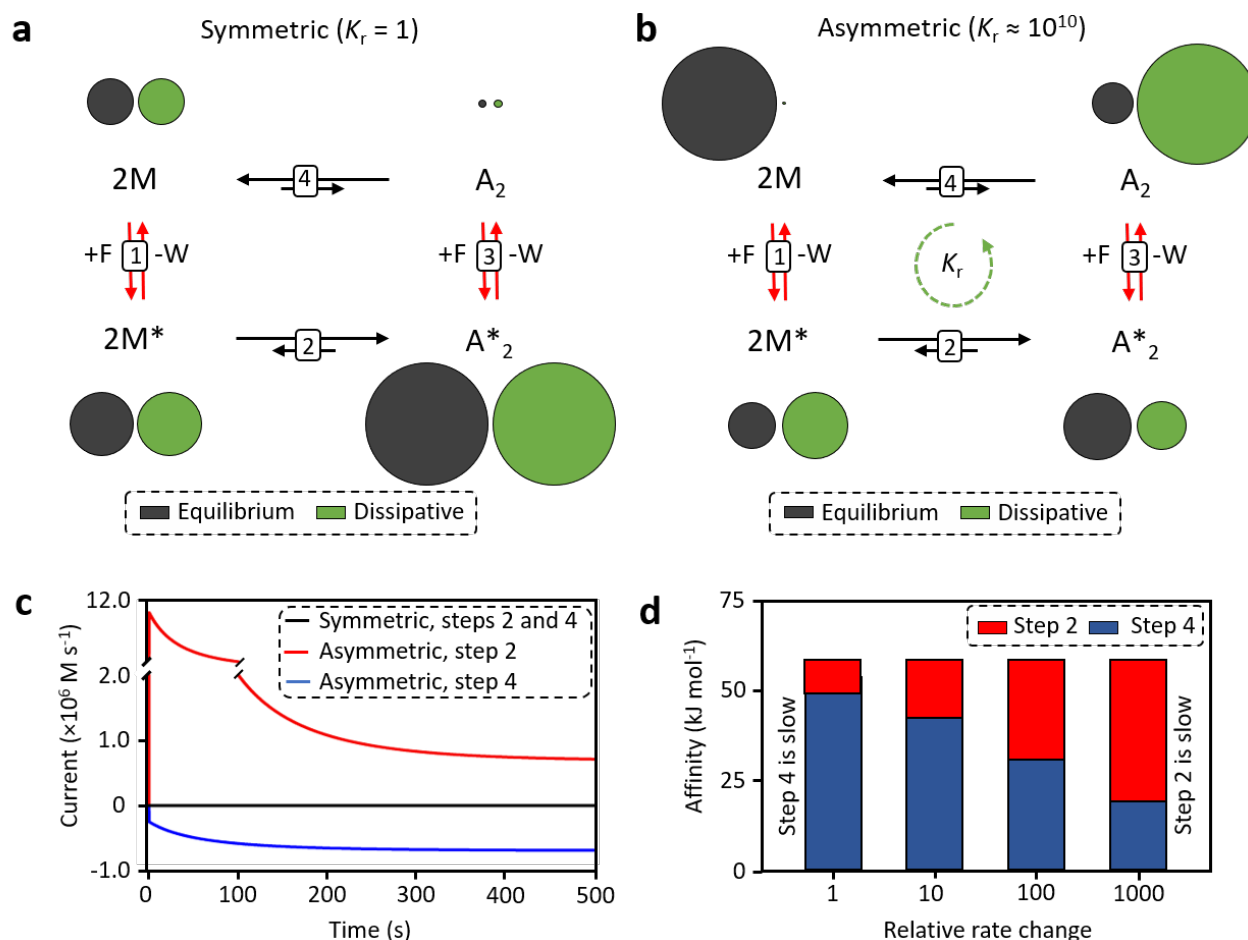


**Fig. 4 | Simulations of dissipative self-assembly processes.** The data reported in this Fig. refers to the model system represented in Fig. 3a for  $n = 2$ ,  $[M]^{\text{TOT}} = 1 \text{ mM}$  and  $[F] = [W] = 1 \text{ M}$  (see text and SI (page 5) for more details) **a**, Steady-state distribution of monomers in the model system in which symmetric energy consumption occurs ( $K_r = 1$ ): green and grey circles correspond to the monomer distribution under dissipative conditions and after equilibration of steps 2 and 4 (same distribution).. **b**, Steady-state distribution of monomers in the model system in which asymmetric consumption occurs ( $K_r \approx 10^{10}$ ): green and grey circles correspond to the monomer distribution under dissipative conditions and after equilibration of steps 2 and 4, respectively. The size of the circles reflects the relative concentrations **c**, Reaction currents monitored in the evolution of model systems described in Fig. 4a, b, from the equilibrium (grey circles) to the dissipative (green circles) state: for the symmetric system (Fig. 4a) currents of step 2 and 4 are superimposed (black line). **d**, Chemical affinity associated to reactions 2 (red) and 4 (blue) in the asymmetric model system of Fig. 4b under steady-state dissipative conditions. The different bars refer to different simulations in which the rate constants of step 2 were gradually decreased and the rate constants of step 4 were gradually increased with the factors indicated on the x-axis.

A crucial distinction between the symmetric and asymmetric case is that only in the latter directionality is present in the system. This phenomenon can be visualized by plotting for steps 2 and 4 the currents, defined as the forward reaction flux minus the backward reaction flux, while the system evolves from thermodynamic equilibrium to the stationary dissipative state (from the grey to green distributions given in Fig. 4b) (Fig. 4c). In the symmetric system (black line) no current arises, because the concentrations do not change. On the contrary, in the asymmetric system a steady state is reached in which the forward, positive current associated to monomer assembly into  $A^*_2$  (step 2 - red line) is perfectly counterbalanced by a backward, negative current associated to the thermodynamically driven disassembly of  $A_2$  (step 4 - blue line). This visualization clearly illustrates that asymmetric consumption of energy provided by the fuel causes the continuous (counterclockwise) cycling of the monomers. In this context, it is of relevance to note that asymmetric consumption of energy is also at the basis of directional movement in

molecular machines, exemplified by the ATP-driven movement of kinesin and dynein along microtubule filaments.<sup>41</sup>

### Energy storage in out-of-equilibrium assemblies

The observation that the system relaxes back to the equilibrium composition when the energy flux is stopped, implies that a certain amount of energy is stored in the system under stationary dissipative conditions. The ability of the system to store part of the consumed energy by populating high-energy structures is a direct consequence of the kinetic asymmetry in the energy consumption pathways. In non-equilibrium thermodynamics, this amount of energy is quantified by chemical affinity, which corresponds to  $-\Delta G$  of an equilibrium under non-standard conditions.<sup>43</sup> In the case of both fast fuel and waste reactions (steps 1 and 3, respectively), the stored energy in the system is described as the energy released in the transition from the dissipative to the equilibrium state and corresponds to the energy associated with the ratcheting constant  $K_r$  ( $\Delta G = -RT \ln K_r$ , amounting to ca. 58 kJ mol<sup>-1</sup> at 298 K and calculated by inserting the used rate constants in equation 2 (see SI (page 4) for details). Thus, the ratcheting constant provides a quantitative tool for measuring to which extent a system is driven out-of-equilibrium. To disclose how the energy is stored in the cycle, we have calculated the chemical affinities for equilibrium steps 2 and 4 under stationary dissipative conditions (Fig. 4d, most left bar). It is shown that nearly all energy is stored in the  $A_2$ -state, which is in line with the fact that the dissociation of  $A_2$  in monomer M was deliberately set as the rate determining step in the cycle. Indeed, the energy is distributed in a different manner in the network when step 4 is accelerated and step 2 is slowed down (10-fold, 100-fold or 1000-fold, Fig. 4d). Although the overall energy stored in the system remains constant, it emerges in a very clear manner that the energy becomes progressively stored in the  $A^*_2$ -state as that aggregate gains in kinetic stability compared to  $A_2$ .

The present discussion highlights two fundamental requirements to obtain and accumulate a high-energy self-assembled structure under constant fuel turnover. First, kinetic asymmetry must be present in the cycle with activation preferentially occurring on the monomer level (M) and deactivation on the aggregate level ( $A^*_n$ ). Second, the high-energy species must be kinetically stable, and the dissociation step should be the kinetic bottleneck in the cycle. These two requirements emerge clearly from the properties of self-assembling microtubules, which are Nature's most prominent structures formed by a chemical fuel driven self-assembly process (Fig. 5).<sup>44</sup> Tubulin-dimers are activated towards self-assembly into microtubules upon complex formation with GTP, but GDP-bound tubulin dimers are not prone to self-assembly. The unique out-of-equilibrium behavior of microtubules stems from the fact that GTP hydrolysis is enormously accelerated in the aggregated state, leading to a GDP-rich – thermodynamically unstable – microtubule.<sup>45,46</sup> In particular, hydrolysis occurs preferentially in the inner part of the growing microtubule, whereas a GTP-rich cap kinetically prevents microtubule disassembly.<sup>47</sup> Catastrophic collapse occurs when the stabilizing cap is lost. It is estimated that an energy of around 21 kJ mol<sup>-1</sup> is stored in GDP-rich microtubules.<sup>48</sup>

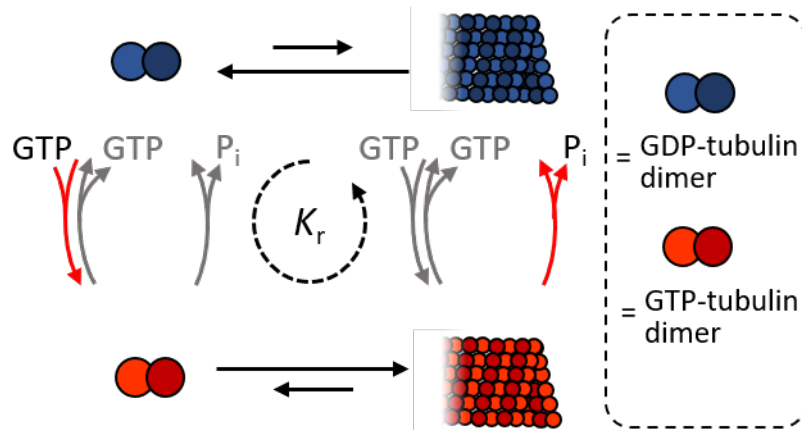


**Fig. 5 | Dissipative self-assembly in Nature.** Reaction scheme for the GTP-driven self-assembly of tubulin dimers. GDP-tubulin dimers are not prone to assembly. However, substitution of guanosine diphosphate (GDP) with guanosine triphosphate (GTP) leads to the formation of GTP-rich microtubules. Hydrolysis of GTP in GDP and inorganic phosphate ( $P_i$ ) in the aggregate is kinetically favored, leading to a high-energy GDP-rich microtubule. Red reactions arrows indicate kinetically preferred pathways, compared to the analogue grey-colored reaction; the notation used for the components is reported in the dashed box. The arrows for the backward waste-reaction is omitted for clarity reasons.

Keeping this natural example of dissipative self-assembly and the above discussion in mind, it is of interest to look again at the general scheme of Fig. 3a. Assuming that the formed waste does not play a significant role in the system ( $k_{1Wf} \ll k_{1Ff}$  and  $k_{3Wf} \ll k_{3Ff}$ ), steps 1 and 3 reduce to the Michaelis-Menten kinetics used to describe enzymatic catalysis. Indeed, the monomers (M) and high energy aggregates ( $A_n$ ) can be interpreted as catalysts for fuel-to-waste conversion through the formation of the activated fuel-catalyst complexes  $M^*$  and  $A_n^*$ , respectively. This interpretation explains why Nature uses enzymes capable of self-aggregation to accomplish self-organization in cells.<sup>49</sup> Aggregation of the enzymes affects the Michaelis-Menten parameters leading to kinetic asymmetry in the energy consumption pathways and, thus, permits the formation of high-energy structures exploiting thermodynamically activated substrates as chemical fuels.<sup>20</sup> This rationalization provides a valuable clue for designing synthetic driven self-assembly processes.

### Dissipative adaptation and evolution

In an asymmetric network, continuous fuel-to-waste conversion is an essential requirement to keep the high-energy assembly state populated. This requirement raises the question of whether kinetic asymmetry in energy consumption can be a selection criterion that determines the composition of a system in which multiple dissipation pathways compete. In the stochastic thermodynamics context of periodically driven systems, England recently proposed that the outcome of a non-equilibrium process might be the state at the end of the trajectory along which the system can absorb and dissipate the largest amount of energy from the external driving force (dissipative adaptation).<sup>50,51</sup> Importantly, this most dissipative state may not necessarily be the most stable one on thermodynamic grounds. Although in this Perspective we deal with macroscopic out-of-equilibrium systems under stationary conditions, the simulations performed in the previous section can be easily extended to show that adaptation is indeed possible in chemically-fueled dissipative self-assembly but only if kinetic asymmetry in energy consumption is present.

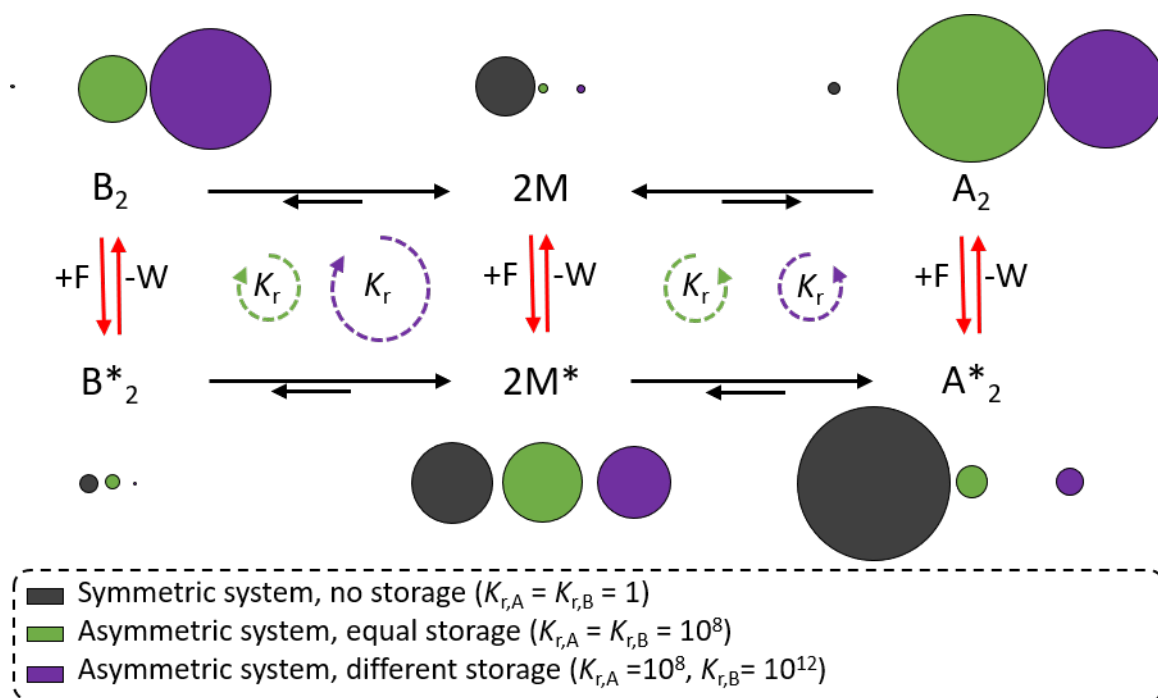


**Fig. 6 | Dissipative adaptation.** Scheme for the association of monomers  $M$  into aggregates  $A_2$  and  $B_2$ ; in the presence of fuel  $F$  the monomer is activated to  $M^*$ , that can assemble into  $A^*_2$  and  $B^*_2$ ;  $B_2$  and  $B^*_2$  are less stable than the corresponding  $A_2$  and  $A^*_2$ . The steady state distribution of monomers is reported according to the  $K_r$  values reported in the legend, for the left and right cycle displaying symmetric energy consumption (no storage, grey circles), equal storage (green circles) and different storage capacity, with the cycle involving  $B_2$  preferred by an amount corresponding to ca.  $23 \text{ kJ mol}^{-1}$  at  $298 \text{ K}$  (purple circles). The size of the circles reflects the relative concentrations of species.

To illustrate this situation, we consider a model in which monomer  $M$  can assemble into two high-energy dimeric aggregates  $A_2$  and  $B_2$ , but  $B_2$  is thermodynamically less stable than  $A_2$  (while having the same kinetic stability) (Fig. 6). Both aggregates can also be formed through fuel-driven pathways that involve the common activated monomer  $M^*$  and the corresponding activated aggregates  $A^*_2$  and  $B^*_2$ . For both cycles the ratcheting constants  $K_{r,A}$  and  $K_{r,B}$ , respectively, can be independently set by adjusting the rate constants of the activation and deactivation steps. In a first simulation, we set both  $K_r$  values 1, implying that the system is not able to store energy (Fig. 6). The calculated distribution of the initial amount of monomer  $M$  over the six possible states (the size of the grey circles) shows that  $M$  resides mostly in the activated states  $A^*_2$  and  $B^*_2$  and that the distribution corresponds to that at thermodynamic equilibrium. This observation implies that energy consumption by itself is not a driving force for adaptation: the crucial factor is the efficiency of the system in storing energy rather than in its capacity to dissipate energy. The same conclusion was recently reached by Astumian in a treatment of dissipative adaptation in the context of stochastic thermodynamics.<sup>38</sup> This conclusion is further supported by a second simulation (green circles), in which the kinetic asymmetry is included in both the  $A_2$ - and  $B_2$ -cycles allowing both cycles to store part of the consumed energy to the same extent ( $K_{r,A} = K_{r,B} = \text{ca. } 1.0 \times 10^8$ ). It can be observed that the high-energy states  $A_2$  and  $B_2$  now become populated at the cost of the activated aggregates  $A^*_2$  and  $B^*_2$ . This observation confirms that kinetic asymmetry installs a ratcheting mechanism. Yet, the higher population of the  $A_2$ - compared to the  $B_2$ -state indicates that, among these high-energy states, the distribution is still reflecting the relative thermodynamic stabilities. The relative distribution changes in the final simulation (purple circles) in which we have further increased the ratcheting constant  $K_{r,B}$  of cycle B (to ca.  $1.0 \times 10^{12}$ ), while keeping the  $K_{r,A}$ -value at the same level. With these new parameters,

the capacity of cycle  $B_2$  to store energy has become higher than that of cycle  $A_2$ . Now, the most populated state in the system becomes  $B_2$ , even if it would be the least populated state under thermodynamic control. These simulations clearly demonstrate that under dissipative conditions the ratcheting strength can become sufficiently dominant to overcome the relative thermodynamic stabilities.

This analysis provides clues on how energy consuming processes may have played an essential role in evolutionary processes. It is tantalizing to imagine that a small mutation in a molecular structure may have led to an improved capacity to store energy, thus opening the energetic pathway towards new forms of self-organization with associated new chemical reactivities. An experimental clue of such a possibility was recently provided by the observation that a 2 base pair mutation in a DNA sequence made the difference whether an energy dissipation process was installed or not.<sup>52</sup> The relevance of kinetic asymmetry leading to ratcheting as an underlying scheme in evolutionary processes<sup>53,54</sup> is further reinforced by the observation that it is also the operating mechanism of molecular machines, of both natural and synthetic origin.<sup>39, 41, 55</sup>

### Perspective & Outlook

In the absence of reported kinetic parameters for all reaction steps in published examples of self-assembling systems relying on chemical fuel consumption,<sup>11,21-36</sup> it is impossible to certify in an unambiguous manner whether these systems exploit a chemically-driven information ratchet mechanism. Such an analysis is further hampered by the fact that most examples rely on the batch-wise addition of fuel, in which high-energy species may indeed be transiently observed, but not necessarily because of asymmetric energy consumption. Yet, the observation of catastrophic events similar to the collapse of those of microtubules seems to provide indirect evidence that an information ratchet may be operative.<sup>11</sup> Indeed, considering the different local environments (pH, polarity, effective concentration)<sup>6</sup> and the possibility of cooperative effects in the aggregated state, it seems unlikely that a certain reaction occurs with the same rate in the monomeric and aggregated state.

Our analysis provides several clues for the experimental design of chemical fuel driven self-assembly processes. The key criterion for pushing a system out-of-equilibrium is the presence of kinetic asymmetry in the dissipative network. This asymmetry can be installed by ensuring that the chemical fuel preferentially binds the monomer rather than the aggregate and/or that fuel-to-waste conversion is more efficiently carried out by the aggregate than by the monomer. Interestingly, both these strategies are present in the operation mechanism of microtubules: the catalytic activity is enhanced in the aggregated state, and part of the waste product is embedded in the high-energy aggregate which disfavors binding of fresh fuel molecules.

Moreover, to maximize energy storage, the kinetics of the equilibrium steps must be slower than the catalytic conversion of fuel, because otherwise the self-assembling steps will rapidly re-equilibrate during fuel-to-waste conversion, in which case all consumed energy is just dissipated without leading to energy storage. It is important to stress that the ratcheting constant  $K_r$  provides a proper quantification of the stored energy only in case of fast fuel-to-waste reactions. This condition implies that the aggregates need to have a significant kinetic stability, a feature that is also beneficial for their observation under the experimental conditions.

Ideally, high-energy aggregates, such as  $A_n$ , should have a spectroscopically distinct fingerprint or an alternative exclusive property compared to the fuel-activated aggregate  $A_n^*$  in order to unambiguously prove their presence in the system and determine their concentrations. Indirect experimental evidence for the occurrence of driven self-assembly in synthetic systems may be obtained from the observation of catastrophic events<sup>11</sup> or the accumulation of aggregates at a concentration not compatible with any equilibrium composition of the system.<sup>4</sup> Although not

definitive, clues that the system operates out-of-equilibrium may also come from a comparison of the systems' properties under dissipative and non-dissipative conditions. Such a difference could be disclosed by suppressing the catalytic activity with inhibitors, or by using substrate-analogs that are not subject to catalysis. Finally, a major effort should be made towards experimental setups that permit determination of the concentration of all species under continuous fuel consumption, rather than under batch-experiments conditions.<sup>33</sup>

Overall, it emerges that kinetic asymmetry leading to ratcheting is a key property to consider when developing chemically-driven out-of-equilibrium assemblies. Apart from novel properties arising from the storage of energy in such assemblies, its successful implementation in synthetic systems will also permit an experimental assessment of the possibility to exploit chemical energy as a driving force for chemical evolution. From this point of view, it is intriguing to observe that processes that on first sight appear very different, such as the directional motion of kinesin or microtubule formation, seem to follow very closely related energy consumption processes.

### Acknowledgments

The authors would like to acknowledge Emanuele Penocchio and Diego Frezzato for insightful discussions. The authors are grateful to Dean Astumian for his help to improve the clarity of the manuscript.

### References

1. Grzybowski, B. A., Huck, W. T. S. The nanotechnology of life-inspired systems. *Nat. Nanotechnol.* **11**, 585-592 (2016).
2. Kassem, S., van Leeuwen, T., Lubbe, A. S., Wilson, M. R., Feringa B. L., Leigh, D. A. Artificial molecular machines. *Chem. Soc. Rev.* **46**, 2592-2621 (2017).
3. Koumura, N., Zijlstra, R. W. J., van Delden, R. A., Harada, N., Feringa, B. L. Light-driven monodirectional molecular rotor. *Nature* **401**, 152-155 (1999).
4. Ragazzon, G., Baroncini, M., Silvi, S., Venturi, M., Credi, A. Light-powered autonomous and directional motion of a dissipative self-assembling system. *Nat. Nanotechnol.* **10**, 70-75 (2015).
5. Cheng, C., McGonigal, P. R., Schneebeli, S. T., Li, H., Vermeulen, N. A., Ke, C., Stoddart J. F. An artificial molecular pump. *Nat. Nanotechnol.* **10**, 547-553 (2015).
6. Wilson, M. R.; Solà, J.; Carlone, A.; Goldup, S. M.; Lebrasseur, N.; Leigh, D. A. An Autonomous Chemically Fuelled Small-Molecule Motor. *Nature* **534**, 235-240 (2016).
7. Erbas-Cakmak, S., Fielden, S. D. P., Karaca, U., Leigh, D. A., McTernan, C. T., Tetlow, D. J., Wilson, M.R. Rotary and linear molecular motors driven by pulses of a chemical fuel. *Science* **358**, 340-343 (2017).
8. Merindol, R., Walther, A. Materials learning from life: concepts for active, adaptive and autonomous molecular systems. *Chem. Soc. Rev.* **46**, 5588-5619 (2017).

9. van Rossum, S. A. P., Tena-Solsona, M., van Esch, J. H., Eelkema, R. Boekhoven, J. Dissipative out-of-equilibrium assembly of man-made supramolecular materials. *Chem. Soc. Rev.* **46**, 5519-5535 (2017).
10. Li, Q., Fuks, G., Moulin, E., Maaloum, M., Rawiso, M., Kulic, I., Foy, J. T., Giuseppone, N. Macroscopic contraction of a gel induced by the integrated motion of light-driven molecular motors. *Nat. Nanotechnol.* **10**, 161-165 (2015).
11. Boekhoven, J., Hendriksen, W., Koper, G., Eelkema, R., van Esch, J. Transient assembly of active materials fueled by a chemical reaction. *Science* **349**, 1075-1079 (2015).
12. Ikegami, T., Kageyama, Y., Obara, K., Takeda, S. Dissipative and autonomous square-wave self-oscillation of a macroscopic hybrid self-assembly under continuous light irradiation. *Angew. Chem. Int. Ed.* **55**, 8239-8243 (2016).
13. Foy, J. T., Li, Q., Goujon, A., Colard-Itté, J. R., Fuks, G., Moulin, E., Schiffmann, O., Dattler, D., Funeriu, D. P., Giuseppone, N. Dual-light control of nanomachines that integrate motor and modulator subunits. *Nat. Nanotechnol.* **12**, 540-545 (2017).
14. Fialkowski, M., Bishop, K. J. M., Klajn, R., Smoukov, S. K., Campbell, C. J., Grzybowski, B. A. Principles and implementations of dissipative (dynamic) self-assembly. *J. Phys. Chem. B.* **110**, 2482-2496 (2006).
15. Grzybowski, B. A., Stone, H. A., Whitesides, G. M. Dynamic self-assembly of magnetized, millimetre-sized objects rotating at a liquid-air interface. *Nature* **405**, 1033-1036 (2000).
16. Krabbenborg, S. O., Veerbeek, J., Huskens, J. Spatially controlled out-of-equilibrium host-guest system under electrochemical control. *Chem. Eur. J.* **21**, 9638-9644 (2015).
17. Göstl, R., Senf, A., Hecht, S. Remote-controlling chemical reactions by light: towards chemistry with high spatio-temporal resolution. *Chem. Soc. Rev.*, **43**, 1982-1996 (2014).
18. Göstl, R., Hecht, S. Controlling covalent connection and disconnection with light. *Angew. Chem. Int. Ed.* **53**, 8784-8787 (2014).
19. Kathan, M., Hecht, S. Photoswitchable molecules as key ingredients to drive systems away from the global thermodynamic minimum. *Chem. Soc. Rev.* **46**, 5536-5550 (2017).
20. Walsh, C. T., Tu, B. P., Tang, Y. Eight kinetically stable but thermodynamically activated molecules that power cell metabolism. *Chem. Rev.* **118**, 1460-1494 (2018).
21. Pezzato, C., Prins, L. J. Transient signal generation in a self-assembled nanosystem fueled by ATP. *Nat. Commun.* **6**, 7790 (2015).
22. Maiti, S., Fortunati, I., Ferrante, C., Scrimin, P., Prins, L. J. Dissipative self-assembly of vesicular nanoreactors. *Nat. Chem.* **8**, 725-731 (2016).

23. Dhiman, S., Jain, A., George, S. J. Transient helicity: fuel-driven temporal control over conformational switching in a supramolecular polymer. *Angew. Chem. Int. Ed.* **56**, 1329-1333 (2017).
24. Dhiman, S., Jain, A., Kumar, M., George, S. J. Adenosine-phosphate-fueled, temporally programmed supramolecular polymers with multiple transient states. *J. Am. Chem. Soc.* **139**, 16568–16575 (2017).
25. Hao, X., Sang, W., Hu, J., Yan, Q. Pulsating polymer micelles via ATP-fueled dissipative self-assembly. *ACS Macro Lett.* **6**, 1151–1155 (2017).
26. Boekhoven, J., Brizard, A., Kowligi, K., Koper, G., Eelkema, R., van Esch, J. Dissipative Self-Assembly of a Molecular Gelator by Using a Chemical Fuel. *Angew. Chem. Int. Ed.* **49**, 4825-4828 (2010).
27. Dambeniaks, A. K., Vu, P. H. Q., Fyles, T. M. Dissipative assembly of a membrane transport system. *Chem. Sci.* **5**, 3396-3403 (2014).
28. Fanlo-Virgós, H., Alba, A. R., Hamieh, S., Colomb-Delsuc, M., Otto, S. Transient substrate-induced catalyst formation in a dynamic molecular network. *Angew. Chem. Int. Ed.* **53**, 11346-11350 (2014).
29. Wood, C. S., Browne, C., Wood, D. M., Nitschke, J. R. Fuel-controlled reassembly of metal–organic architectures. *ACS Cent. Sci.* **1**, 504–509 (2015).
30. Tena-Solsona, M., Rieß, B., Grötsch, R., Löhner, F., Wanzke, C., Käsdorf, B., Bausch, A., Mueller-Buschbaum, P., Lieleg, O., Boekhoven, J. Non-equilibrium dissipative supramolecular materials with a tunable lifetime. *Nat. Commun.* **8**, 15895 (2017).
31. Kariyawasam L. S., Hartley, C. S. Dissipative assembly of aqueous carboxylic acid anhydrides fueled by carbodiimides. *J. Am. Chem. Soc.* **139**, 11949–11955 (2017).
32. Sawczyk, M., Klajn, R. Out-of-Equilibrium Aggregates and Coatings during Seeded Growth of Metallic Nanoparticles. *J. Am. Chem. Soc.* **139**, 17973–17978 (2017).
33. Sorrenti, A., Leira-Iglesias, J., Sato, A., Hermans, T.M. Non-equilibrium steady-states in supramolecular polymerization. *Nat. Commun.* **8**, 15899 (2017).
34. van Ravensteijn, B. G. P., Hendriksen, W. E., Eelkema, R., van Esch, J. H., Kegel, W. K. Fuel-mediated transient clustering of colloidal building blocks. *J. Am. Chem. Soc.* **139**, 9763-9766 (2017).
35. Mishra, A., Korlepara, D. B., Kumar, M., Jain, A., Jonnalagadda, N., Bejagam K. K., Balasubramanian S., George, S. J. Biomimetic tempolar self-assembly via fuel-driven controlled supramolecular polymerization. *Nat. Commun.* **9**, 1295 (2018).
36. Della Sala, F., Maiti, S., Bonanni, A., Scrimin, P., Prins, L. Fuel-selective transient activation of nanosystems for signal generation. *Angew. Chem. Int. Ed.* **130**, 1611-1615 (2018).

37. Astumian, R. D. Stochastic conformational pumping: a mechanism for free-energy transduction by molecules. *Annu. Rev. Biophys.* **40**, 289-313 (2011).
38. Astumian, R. D. Stochastic pumping of non-equilibrium steady-states: how molecules adapt to a fluctuating environment. *Chem. Commun.* **54**, 427-444 (2018).
39. Astumian, R. D. Design principles for Brownian molecular machines: how to swim in molasses and walk in a hurricane. *Phys. Chem. Chem. Phys.* **9**, 5067–5083 (2007).
40. Alvarez-Pérez, M., Goldup, S. M., Leigh, D. A., Slawin, A. M. Z. A chemically-driven molecular information ratchet. *J. Am. Chem. Soc.* **130**, 1836-1838 (2008).
41. Astumian, R. D. Microscopic reversibility as the organizing principle of molecular machines. *Nat. Nanotechnol.* **7**, 684-688 (2012).
42. Rao, R., Esposito, M. Nonequilibrium thermodynamics of chemical reaction networks: wisdom from stochastic thermodynamics. *Phys. Rev. X* **6**, 041064 (2016).
43. Kondepudi, D., Prigogine, I. Modern thermodynamics: from heat engines to dissipative structures. John Wiley & Sons, Ltd (1998).
44. Hess, H., Ross, J. L. Nonequilibrium assembly of microtubules: from molecules to autonomous chemical robots. *Chem. Soc. Rev.* **46**, 5570-5587 (2017).
45. David-Pfeuty, T., Erickson, H. P., Pantaloni, D. Guanosinetriphosphatase activity of tubulin associated with microtubule assembly. *Proc. Nat. Acad. Sci. USA* **74**, 5372-5376 (1977).
46. Caplow, M., Shanks, J. Mechanism of the microtubule GTPase reaction. *J. Biol. Chem.* **265**, 8935-8941 (1990).
47. Bowne-Anderson, H., Zanic, M., Kauer, M., Howard J. Microtubule dynamic instability: a new model with coupled GTP hydrolysis and multistep catastrophe. *Bioessays* **35**, 452-461 (2013).
48. Desai, A., Mitchison, T.J. Microtubule polymerization dynamics *Annu. Rev. Cell Dev. Biol.* **13**, 83-117 (1997).
49. Epstein, I. R., Xu, B. Reaction-diffusion processes at the nano- and microscales. *Nat. Nanotechnol.* **11**, 312-319 (2016).
50. England, J. L. Dissipative adaptation in driven self-assembly. *Nat. Nanotechnol.* **10**, 919-923 (2015).
51. Perunov, N., Marsland, R. A., England, J. L. Statistical physics of adaptation. *Phys. Rev. X* **6**, 021036 (2016).

52. Del Grosso, E., Amodio, A., Ragazzon, G., Prins, L., Ricci, F. Dissipative synthetic DNA-based receptors for the transient load and release of molecular cargo. *Angew. Chem. Int. Ed.*, in press, DOI: 10.1002/anie.201801318.
53. Hoffmann, P. M. Life's ratchet. Basic Books (2012).
54. Branscomb, E., Biancalani, T., Goldenfeld, N., Russell, M. Escapement mechanisms and the conversion of disequilibria; the engines of creation. *Phys. Rep.* **677**, 1-60 (2017).
55. Erbas-Cakmak, S., Leigh, D. A., McTernan, C. T., Nussbaumer, A. L. Artificial molecular machines. *Chem. Rev.* **115**, 10081-10206 (2015).